Resolution Improvement of an UWB Microwave Imaging Radar System Using Circular Polarization

Richard Torrealba-Meléndez, José L. Olvera-Cervantes, and Alonso Corona-Chávez
Instituto Nacional de Astrofísica, Óptica y Electrónica, INAOE.
rtorreal@ieee.org

***Abstract*—An ultra-wideband (UWB) microwave imaging radar system with a circularly polarized antenna is presented. The proposed microwave imaging system operated in the full UWB spectrum (3.1 to 10.6GHz). To verify the performance and resolution improvement of our system, two experimental tests were developed. Furthermore a comparison between linear polarization (LP) and circular polarization (CP) was carried out. Using circular polarization has demonstrated to improve the depth resolution of the UWB microwave imaging radar systems. In addition circular polarization provides a good approximation of the shape and size of the objects.**

Keywords—Circular polarization, Ultra wideband (UWB), microwave imaging

I. INTRODUCTION

Ultra-wideband (UWB) microwave imaging radar has many potential applications such as; medical imaging, through- the-wall imaging, security imaging and others [1] -[4]. All this requires real time with good resolution and the ability to penetrate opaque lossy dielectric materials (such as biological tissues, concrete, plastic, ceramic, drywall, or other dielectrics). In order to improve resolution, the Ultra-wide band (UWB) standard (3.1 GHz to 10.6 GHz) offers a good solution as more than 7 GHz of instant bandwidth are available [5].

However, like all radar systems, UWB radar suffer from fading radar cross section (RCS) caused by the orientation and composition of the objects, the fading RCS reduce considerably the resolution of the system. The fading RCS problem in a radar imaging system is due to the use of linearly polarized (LP) antennas for transmission and reception. Electromagnetic scattering in LP systems for naturally occurring objects, which often have multiple boundaries of different materials, shapes, and sizes, tend to have a change of polarization at the interfaces. Hence, the receiver antenna does not have a natural alignment to the polarization angle of the scattered wave. One way to reduce the fading RCS and improve the resolution of these systems is included polarization diversity [6] -[8]. To obtain polarization diversity circularly polarized antennas can be used as shown in [9]. Circularly polarized antennas can improve the performance of UWB microwave imaging radar systems in two ways; the first is that we can achieve an improvement in the ability to penetrate lossy dielectric materials [10]. The second is polarization losses, this polarization mismatch could reach ∞dB (no power extracted by the antenna). However using circular polarization in the system polarization losses are limited to 3dB [11]. With the improvement of these two points, we can get the most amount of information of the scenario under inspection. To date, no system has been found by the authors showing circular polarization in the full UWB spectrum used for microwave radar imaging. In [12] imaging radars are presented with a maximum of 50% of total BW. It is only recently that circularly polarized antennas can provide good axial ratios (AR) across the full UWB frequency range [13].

This work presents an UWB microwave imaging radar with circularly polarized antennas in the full UWB spectrum. It will be experimentally demonstrated that the use of circular polarization improves the resolution of the UWB microwave imaging radar systems compared to vertical and horizontal polarizations.

II. EXPERIMENTAL UWB MICROWAVE IMAGING RADAR SYSTEM

The configuration of the proposed mono-static UWB microwave imaging radar system is shown in Fig. 1. This is formed by a mechanical system that controls the position of the antenna on the azimuth axis (x- axis) in steps of 1cm. The antenna used in this work is circularly polarized and operates in the full UWB frequency range, the antenna is connected to a SPARQ-3002E Lecroy vector network analyzer which measure the reflection coefficient (*S11*), with frequency steps of 5MHz. Finally the data processing is performed on a computer.

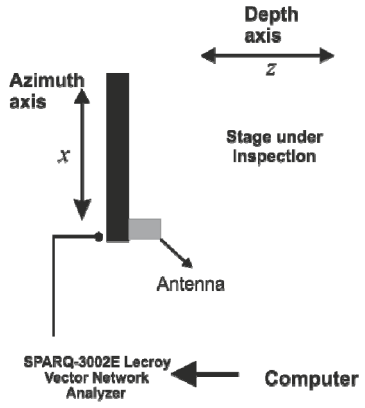

Fig. 1. Configuration of UWB microwave radar imaging radar system.

A. IMAGING ALGORITHM

First all the measures need to be calibrating, to do that the system need a measure without object. In addition, the following equation is applied (1) [3]

$$S11_C(x_n, f) = S11_O(x_n, f) - S11_{WO}(f) \quad (1)$$

Where $S11_O$ is the reflected field with the object, and $S11_{WO}$ is reflected field without the object and x_n denote the *n-position* in *x (n=1, 2, 3…N)*. With this calibration we can remove undesired reflection caused by cables, the feeding network and antenna. Next, a zero padding and Hamming window are applied to every measurement [3]. Hamming window eliminates undesired reflections and zero padding enhances the resolution of the inverse Fourier transform (IFT). The IFT is used to transform the measured reflection coefficients in time domain. A delay time correction is done to get the right object positions [3]. The reflection coefficients in the time domain are grouped in a matrix *I* with dimensions (*M×N)*, where M denotes the points used to compute the IFT and N is the number of measurements in the azimuth axis. Finally to get the image the Kirchhoff's migration is applied to eliminate the hyperbolic curves effect originated by the scatters and so obtain the image [14]. Fig. 2 shows a flowchart of the image algorithm.

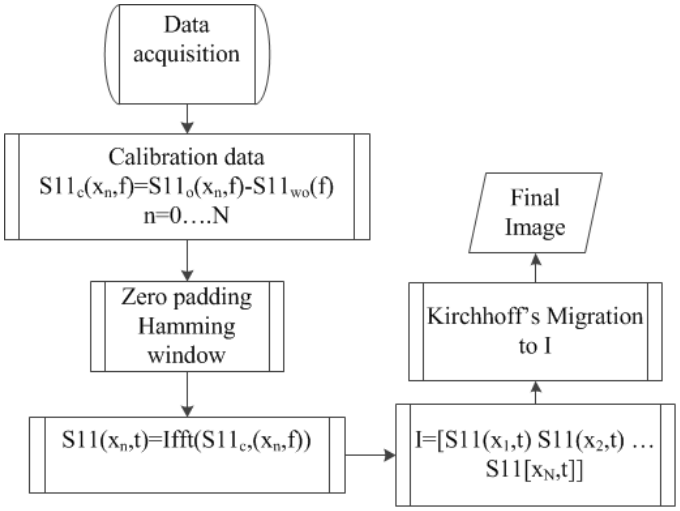

Fig. 2. Flowchart of the image algorithm

B. CIRCULAR POLARIZED ANTENNA

The proposed circularly polarized antenna is composed of a feed network and an array of four Vivaldi antennas. The Schematic of the feed network and antenna array is shown in Fig. 3.

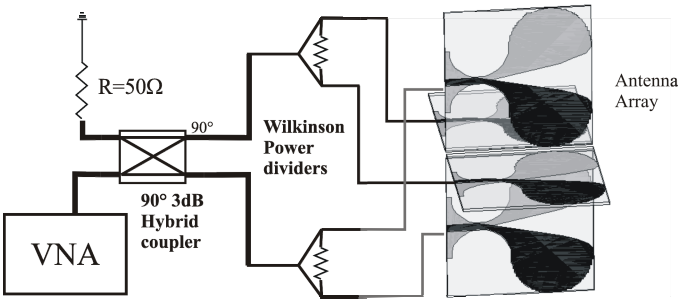

Fig. 3. Schematic of the feed network and antenna array.

The feed network consists of a 90° 3dB hybrid coupler and two Wilkinson power dividers. The proposed circularly polarized antenna is constructed using an array of four linear polarized (LP) elliptically tapered antipodal Vivaldi's antennas [15]. The antenna array has a cross arranged as shown in Fig 3. The substrate used for the design is 1.58-mm-thick Rogers 4003C and size of one antenna is 8 cm X 8 cm. Fig. 4, shows the measured return loss (S11) of the antenna array, which is better than -10dB from 1.4 to 10.6 GHz. The measured axial ratio is illustrated in Fig. 5. The axial ratio is below 3dB in the full UWB frequency range.

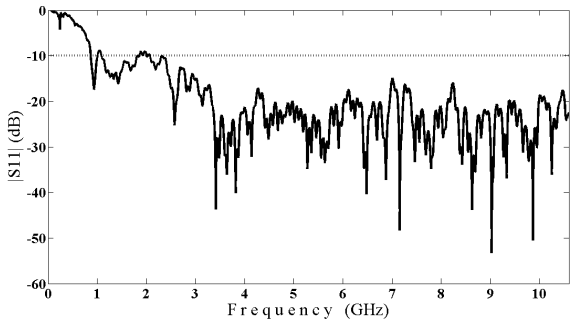

Fig. 4. Measured return loss (S11)

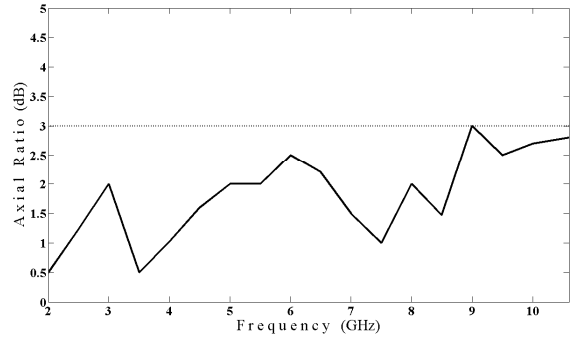

Fig. 5. Measured axial ratio.

III. MEASUREMENT RESULTS

To verify the capabilities of circular polarization in an UWB microwave imaging radar, we proposed two complex experimental setups. These experimental setups are composed

with objects which have different parameters of permittivity (εr) and conductivity (σ). The first setup is presented in Fig. 6, this consists of a 10cm thick a brick wall (εr=5, σ=0.12 S/m) with a plastic pipe full of water (εr=81, σ=0.05 S/m) and copper pipe (σ=5.9x10^7 S/m) behind it. The measurements were carried out inside an anechoic chamber to prevent undesired reflections from the environment. It is worth noting that the reflections from the wall were removed in the calibration.

Given that the microwaves are very sensitive to the dielectric contrast, in this experiment we expected to detect the water pipe and copper pipe with clarity, this because the reflection coefficient to the water with an incident angle $\theta_i=0$ is Γ_w=0. 8 and the reflection coefficient to the copper is Γ_c=1, these coefficients were obtained using the following equation:

$$\Gamma = \frac{\eta_2 - \eta_1}{\eta_2 + \eta_1} \qquad (2)$$

Where η1 is the impedance intrinsic of the air and η2 is the impedance intrinsic of the water or copper, both impedances are related to permittivity and permeability to the medium as $\eta = \sqrt{\mu/\varepsilon}$.

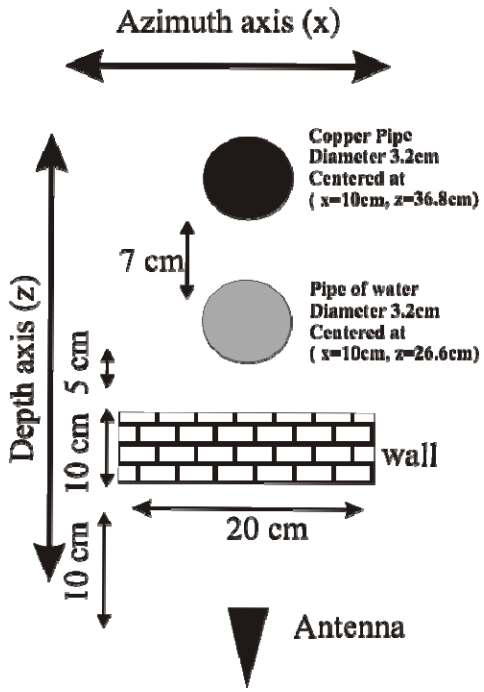

Fig. 6. First experimental setup. The antenna was placed at 10cm of the wall, behind this wall at a distance of 5 cm was placed a plastic pipe full of water with a diameter of 3.2cm, behind this pipe with water at a distance of 7cm was placed a pipe of copper with the same dimension as plastic pipe.

In order to demonstrate that circular polarization improves the resolution of the system, three images in two dimensions (azimuth x-axis, depth y-axis) were obtained, one with circular polarization (CP) and two more with vertical (VP) and horizontal (HP) polarization. The images with vertical and horizontal polarization were obtained using one Vivaldi antenna. Fig. 7 shows the images obtained for this first setup.

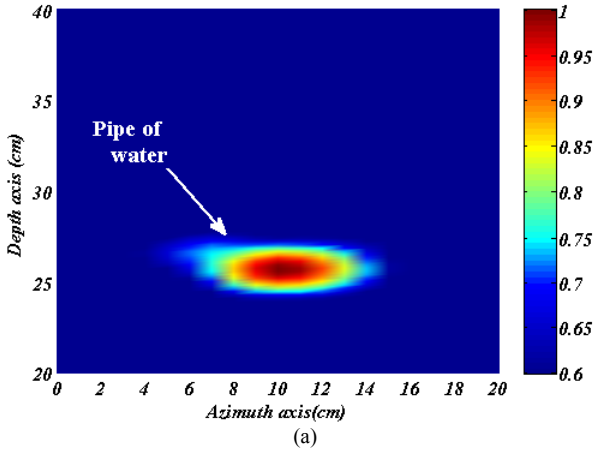

(a)

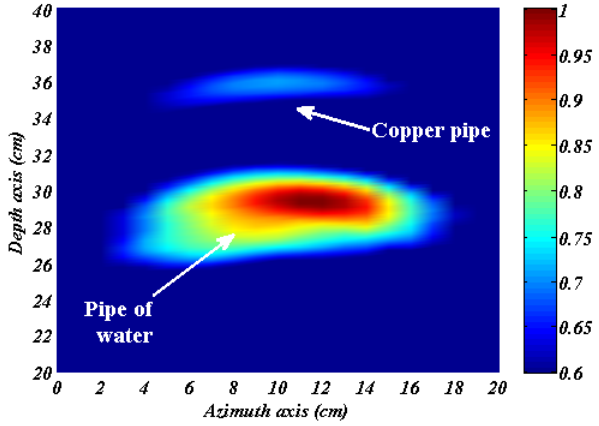

(b)

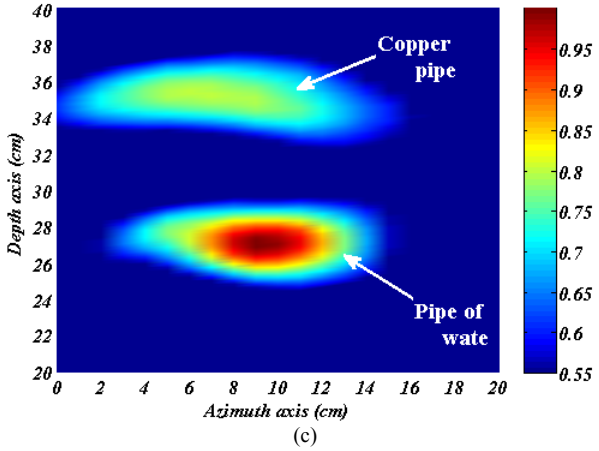

(c)

Fig. 7. 2D imaging results for the first experimental setup. (a) Image with VP (b) Image with HP, (c) Image with CP.

The imaging obtained with vertical polarization, Fig. 7 (a), only can see the pipe of water. For horizontal polarization the copper pipe is barely visible [Fig. 7 (b)]. Whereas for circular polarization [Fig. 7(c)] the two pipes are clearly distinguished. From the result images we obtain the dimensions of the pipes

in azimuth and depth axis for the three polarizations, also we obtain the contrast difference between pipes and the background. This is shown in the Table I.

Table I.
MEASUREMENTS OF OBJECTS DIMENSIONS AND CONTRAST DIFFERENCES.

	Azimut Axis		Depth Axis		Contrast difference between pipes	Contrast difference Between copper pipe and background
	Water	Copper	Water	Copper		
VP	5cm	-	3cm	-	-	-
HP	9cm	8cm	5cm	2cm	0.3	0.1
CP	7cm	8cm	4cm	3.5cm	0.2	0.35

To the Table I we can observe that the circular polarization improves the resolutions of the system in the depth axis, the dimension in this axis for the water and copper pipes are close to the real dimensions. On the other hand the contrast between difference the pipes for CP is 0.2 and for HP this contrast difference increase to 0.3. Finally the contrast between empty space and the copper pipe is only about 0.1 for horizontal polarization and for the circular polarization the empty space-second pipe contrast is over 0.35, more than double than horizontal polarization. With this result we can show that the circular polarization improves the resolution in the depth axis and also improve the RCS for this system in comparison with linear polarization.

In the second scenario, Fig. 8 the plastic and copper pipes were replaced by a plastic container of oil ($\varepsilon r=3$, $\sigma \approx 0$ S/m) with a diameter of 10 cm and a height of 15cm, in the center of this container a copper pipe was placed with the same height and a diameter of 3.2cm. According to equation (2), the reflection coefficient of the oil is $\Gamma_{oil}=0.33$. As in the first example three images were obtained (HP, VP and CP). The results are shown in Fig 9.

In Figs 9 (a) and 9 (b), we can see the interface air-oil and distinguish the copper pipe but with a poor resolution in the shape of copper pipe. However the image obtained using circular polarization, Fig. 9 (c) shows an improvement in resolution. We can see in this image that the shape of copper pipe is well defined. Furthermore in Fig. 9 (c) we can observe that the size of the oil container in the depth axis is close to 10cm. Moreover the copper pipe has a 4cm of diameter in

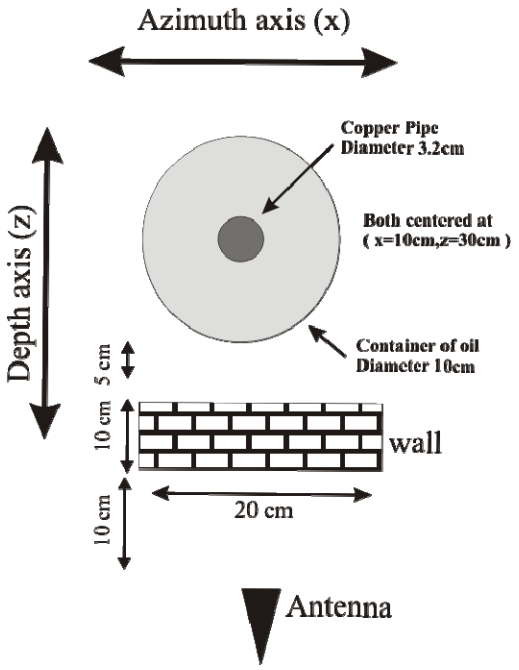

Fig. 7. Second experimental setup. In this setup the plastic pipe and the copper pipe were replaced by a plastic container of oil with a diameter of 10 cm and a height of 15cm, in the center of this container was placed a copper pipe with the same height and a diameter 3.2cm.

depth and azimuth axis. For vertical and horizontal polarizations the depth resolution of the oil container is only about 5cm and the copper pipe is 3cm. Besides size obtained in azimuth axis of the copper pipe is close to 10 cm for linear polarization. In the Table II we show a comparison between the three polarizations related to the size of the copper pipe.

Table II.
MEASUREMENTS OF THE COPPER PIPE DIMENSIONS

Polarization	Depth axis	Azimuth axis
VP	3cm	10cm
HP	3cm	10cm
CP	4cm	4cm

These two experiments show that circular polarization; improves the depth resolution. This is because in circular polarization, there is greater penetration into the material in comparison with linear polarizations. Moreover, it was demonstrated that with circular polarization the shape and size of the object with respect to the depth axis are better defined in both axis.

It is important to highlight that to generate circular polarization in this work the input power is divided in two by the hybrid coupler, and even then the results obtained with this polarization are better than those obtained with the linear polarizations.

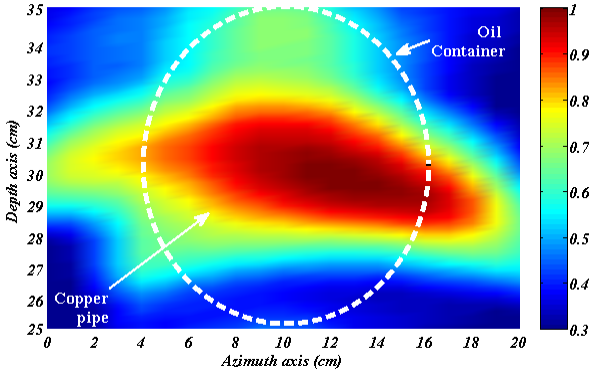

(a)

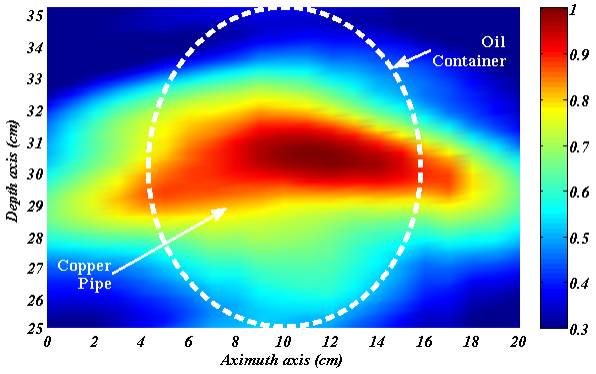

(b)

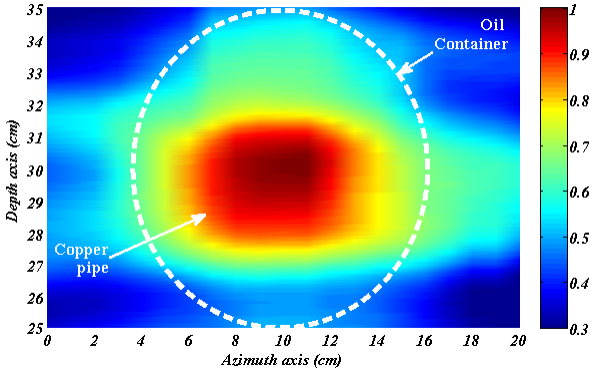

(c)

Fig. 9. 2D imaging results for the second experimental setup. (a) Image with VP (b) Image with HP, (c) Image with CP.

Finally Table III presents a comparison between various UWB radar imaging systems.

Table III.
COMPARISION OF UWB RADAR IMAGING SYSTEMS

Reference	Polarization	Frequency Range	Dielectric Object Detection	Metal Object Detection
[3]	Linear	3.1-10.6 GHz	No	No
[8]	Dual	0.7-3.1 GHz	Yes	Yes
[12]	Circular	6-10 GHz	No	Yes
This Work	Circular	3.1-10.6 GHz	Yes	Yes

IV. CONCLUSION

An UWB microwave imaging radar with circularly polarized antenna has been presented. The system has been tested in two experimental examples. The presented results have demonstrated that circular polarization improves the resolution of the UWB microwave imaging radar. Both depth penetration resolution and the determination of the size and shape of the object were improved compared to LP.

REFERENCES

[1] M. Klemm, J.A. Leendertz, D. Gibbins, I. J. Craddock, A. Preece, and R. Benjamin., "Microwave Radar-Based Breast Cancer Detection: Imaging in Inhomogeneous Breast Phantoms," *IEEE Antenna Wireless Propag. Lett.,* Vol. 8, pp. 1349-1352, Nov. 2009.

[2] Q. Huang; L. Qu, B. Wu, and F. Guangyou, "UWB Through-Wall Imaging Based on Compressive Sensing," *IEEE Trans. Geosci. and Remote Sens.,* Vol. 48, no. 3, pp. 1408-1415, Mar. 2010.

[3] C. R. P. Dionisio, S. Tavares , M. Perotoni, S. Kofuji., "Experiments on through-wall imaging using ultra wideband radar," *Microw. and Opt. Tech. Lett.*, vol. 54, no 2, pp. 339–344, Feb. 2012.

[4] L. Jofre,; A. Broquetas, J. Romeu, S. Blanch, A.P. Toda, X. Fabregas and A. Cardama, "UWB Tomographic Radar Imaging of Penetrable and Impenetrable Objects," *Proc. IEEE*, vol. 97, no.2, pp. 451-464, Feb. 2009.

[5] Federal Communications Commission FCC 02-48, 2002.

[6] A. Sabouni, and A.A. Kishk, "Dual-Polarized, Broadside, Thin Dielectric Resonator Antenna for Microwave Imaging," *IEEE Antennas Wireless Propag. Lett.,* vol. 12, pp. 380-383, Mar. 2013.

[7] G. Adamiuk, T. Zwick, and W. Wiesbeck, "Compact, Dual-Polarized UWB-Antenna, Embedded in a Dielectric," *IEEE Trans. Antennas and Propag.*, vol. 58, no. 2, pp. 279-286, Feb. 2010.

[8] C. Debes, A.M. Zoubir, and Amin, M.G., "Enhanced Detection Using Target Polarization Signatures in Through-the-Wall Radar Imaging," *IEEE Trans. Geosci. and Remote Sens.*, vol. 50, no. 5, pp. 1968-1979, May 2012

[9] X.L. Bao and M.J. Ammann, "Printed circularly polarized antenna with ultra-wide axial-ratio bandwidth," IET *Microwaves, Antennas Propag.,* vol. 5, no .9, pp.1089-1096, June 27 2011.

[10] J. Thaysen, K. B. Jakobesen and J. Appel-Hansen "Circular Polarized Stepped Frequency Ground-Penetrating Radar for Humanitarian demining," in *Proc. SPIE 4394, Detection and Remediation Technologies for Mines and Minelike Targets VI,* 671, October 2001.

[11] C. A. Balanis, "*Antenna Theory Analysis and Desing,*" Third edition, John Wiley and Sons, New Jersey, 2005.

[12] V.G Semenchik,V.I. Deminchik, and V.A. Pahomov, "Using circularly polarized waves for small elongated objects detection in microwave imaging," in *CriMiCo 2009.,* 14-18 Sept. 2009. pp .955-,956.

[13] S.G. Mao, J.C. Yeh, and S.L. Chen, "Ultrawideband Circularly Polarized Spiral Antenna Using Integrated Balun With Application to Time-Domain Target Detection," *IEEE Trans. Antennas and Propag.*, vol. 57, no. 7, pp. 1914-1920, July 2009.

[14] C. Ozdemir, S. Demirci, and E. Yigit, "Practical algorithms to focus b-scan GPR images: theory and application to real data," *Progress In Electromagnetics Research B*, Vol. 6, 109-122, 2008.

[15] E.P Li, H.S Li; J.M. Cai, "The conformal finite-difference time-domain analysis of the antipodal Vivaldi antenna for UWB applications," *in ISAPE '06*. 26-29 Oct. 2006. pp.1-4.